The compressibility mechanism of $Li_3Na_3In_2F_{12}$ garnet

2006 J. Phys.: Condens. Matter 18 2915

(http://iopscience.iop.org/0953-8984/18/10/014)

INSTITUTE OF PHYSICS PUBLISHING JOURNAL OF PHYSICS: CONDENSED MATTER

J. Phys.: Condens. Matter **18** (2006) 2915–2924 doi:10.1088/0953-8984/18/10/014

The compressibility mechanism of $Li_3Na_3In_2F_{12}$ garnet

Andrzej Grzechnik[1,4], Tonci Balic-Zunic[2], Emil Makovicky[2], Jean-Yves Gesland[3] and Karen Friese[1]

[1] Departamento de Física de la Materia Condensada, Universidad del País Vasco, Apartado 644, Bilbao, E-48080, Spain
[2] Geological Institute, University of Copenhagen, 1350 Copenhagen, Denmark
[3] Université du Maine-Cristallogenese, F-72025 Le Mans cedex, France

E-mail: andrzej@wm.lc.ehu.es

Received 14 November 2005
Published 20 February 2006
Online at stacks.iop.org/JPhysCM/18/2915

Abstract

The high pressure behaviour of $Li_3Na_3In_2F_{12}$ garnet ($Ia\bar{3}d$, $Z = 8$) is studied up to 9.2 GPa at room temperature in diamond anvil cells using x-ray diffraction. Its equation of state to 9.2 GPa and the pressure dependences of the structural parameters to 4.07 GPa are determined from synchrotron angle-dispersive powder and laboratory single-crystal data, respectively. No indication of any structural phase transition in this material has been found up to 9.2 GPa. The fitting of the Murnaghan equation of state yields $B_0 = 36.2(5)$ GPa, $B' = 5.38(18)$, and $V_0 = 2051.76(0.69)$ Å^3. The compressibility mechanism of $Li_3Na_3In_2F_{12}$ is attributed to the substantial bending of the In–F–Li angles linking the InF_6 octahedra and LiF_4 tetrahedra. The most compressible polyhedral units are the NaF_8 triangulated dodecahedra. These results are discussed in relation to previous high pressure photoluminescence measurements and compared with the high pressure behaviour of silicate garnets.

(Some figures in this article are in colour only in the electronic version)

1. Introduction

The crystal structure of $M'_3M''_3M'''_2X_{12}$ (X = O, F, OH) garnets ($Ia\bar{3}d$, $Z = 8$) is a three-dimensional framework with each $M'''O_6$ octahedron joined to six others through vertex-sharing $M'X_4$ tetrahedra [1]. Cations M″ occupy eightfold (triangulated dodecahedra or bisdisphenoids) interstitial positions in this framework. In fluoride garnets, the M′ and M″ cations are lithium and sodium, respectively, while the M‴ cations can be trivalent group III or transition metal ions (figure 1) [2–8]. Measurements of magnetic susceptibilities in the

[4] Author to whom any correspondence should be addressed.

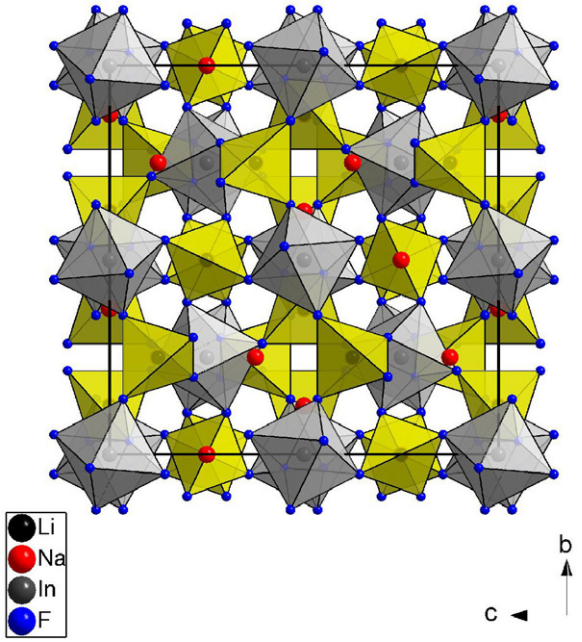

Figure 1. Crystal structure of $Li_3Na_3In_2F_{12}$ garnet ($Ia\bar{3}d$, $Z = 8$).

compounds containing Cr^{3+}, Ti^{3+}, and Fe^{3+} show antiferromagnetic order at approximately 0.13 K, 11 mK, and 0.8 K, respectively [9]. A sudden drop in susceptibility occurs below about 75 and 30 mK for $Li_3Na_3Fe_2F_{12}$ and $Li_3Na_3Cr_2F_{12}$, respectively, possibly indicating the existence of low temperature polymorphs.

The fluoride garnets doped with trivalent ions (mostly Cr^{3+} ions) at the octahedral sites are materials for tunable lasers [10–17]. The crystalline field at their octahedral site could be changed by varying the M‴ cations. For large M‴ cations, the crystalline field is weak and Cr^{3+} luminescence spectra show a wide emission band [12, 17]. The variation of the crystalline field could also be studied through spectroscopic measurements under high pressures without any need to chemically substitute cations in the garnet structure. De Viry *et al* [12] measured photoluminescence in Cr^{3+}-doped $Li_3Na_3In_2F_{12}$ to 12.5 GPa and found that the increase in the exponential lifetime of the $^4T_2$ emission was due to the low–high crystal field transition. A new emission attributed to the ^2E level appeared at 4 GPa, with the crossing between the $^4T_2$ and ^2E levels at 5.9 GPa.

This work has been undertaken to investigate the compressibility mechanism of $Li_3Na_3In_2F_{12}$ garnet. We have used x-ray diffraction to study both powder samples and single crystals of this material to determine its equation of state and the pressure dependences of various structural parameters, respectively. Our results are discussed in relation to spectroscopic observations by de Viry *et al* [12]. We also compare the compression in $Li_3Na_3In_2F_{12}$ to that in silicate garnets [18, 19].

2. Experimental details

A single crystal of $Li_3Na_3In_2F_{12}$ (previously studied in [17]) was pulled from a stoichiometric melt using the Czochralski method. Part of it was finely ground and loaded into a Betsa

membrane diamond anvil cell for high pressure angle-dispersive powder x-ray diffraction measurements to 9.2 GPa on the Swiss–Norwegian Beamlines at the European Synchrotron Radiation Facility (BM1A, ESRF, Grenoble, France). Monochromatic radiation at 0.7100 Å was used for data collection on an image plate MAR345. The images were integrated with the program FIT2D [20] to yield intensity versus 2θ diagrams. The ruby luminescence method [21] was used for pressure calibration.

A series of x-ray single-crystal intensity measurements was performed at high pressures on another fragment of the same crystal (approximately 100 μm × 80 μm × 50 μm) using a CCD-equipped Bruker AXS four-circle diffractometer with graphite-monochromatized Mo Kα radiation. The diamond cell was of the Diacell DXR-6 type (with the opening angle of 90°), the diamonds had culets of 600 μm, and a 300 μm hole was drilled into a stainless steel gasket preindented to a thickness of about 100 μm. The intensities were collected upon compression. The integrated intensities were extracted and corrected for absorption using the Bruker software [22]. Since a ruby luminescence system for pressure calibration was not available to us during our single-crystal measurements, the pressures were determined from the equation of state obtained from the x-ray powder data (figure 2). Errors in the lattice parameter of $Li_3Na_3In_2F_{12}$, for instance due to the decentring of the crystal on the CCD system, would lead to an error in the pressures determined. However, any additional pressure marker [23], like quartz or fluoride, would also suffer from the same effect and would not allow us to obtain a more reliable pressure calibration. The 1:4 mixture of ethanol:methanol was used as a hydrostatic pressure medium during both the powder and the single-crystal measurements.

3. Results

Figure 2 shows selected x-ray powder patterns at different pressures. The ambient pressure lattice parameter and unit-cell volume of $Li_3Na_3In_2F_{12}$ garnet studied here are $a_0 = 12.7070(14)$ Å and $V_0 = 2051.76(69)$ Å^3, respectively. The unit-cell volumes vary smoothly with pressure and do not show any anomaly that might be associated with a structural phase transition (figure 3). They could be fitted up to 9.2 GPa by a Murnaghan equation of state, giving a zero-pressure bulk modulus $B_0 = 36.2(5)$ GPa, and a first pressure derivative of the bulk modulus $B' = 5.38(18)$ with fixed $V_0 = 2051.76(69)$ Å^3.

The refinements of the single-crystal data collected at high pressures have been made with the program JANA2000 [24]. Experimental data and structural parameters[5] are given in tables 1–3. The initial structural model in space group $Ia\bar{3}d$ ($Z = 8$) for all the refinements consisted of the In and Na atoms at special positions 16a (0, 0, 0) and 24c (0.125, 0, 0.25), respectively. The positions Li and F atoms have been determined from the difference $F_{obs} - F_{calc}$ Fourier synthesis. The Li atom is at the special position 24d (0.375, 0, 0.25), while the F atom has been located at the general site 96h (x, y, z). The displacement parameters for Na, In, and F (unlike those for Li) have been refined anisotropically. An isotropic Gaussian extinction correction (G_{iso}) has also been applied [25].

The fluorine coordinates x and z stay basically constant and only the y coordinate shows a clear increase with increasing pressure (table 1), resulting in a strong folding of the In–F–Li angle between the InF_6 and LiF_4 polyhedra that constitute the three-dimensional structure of $Li_3Na_3In_2F_{12}$ garnet (figures 1 and 3). The absolute change in this angle is about 3° upon compression to 4.07 GPa. The change in the y coordinate also implies a decrease of the Na–F(1) distance, while the three remaining bonds between the fluorine atoms and the nearest

[5] Further details of the crystallographic investigations can be obtained from the Fachinformationszentrum Karslruhe, D-76344 Eggenstein-Leopoldshafen, Germany, on quoting the depository numbers CSD 416180-416185.

Table 1. Experimental data for single-crystal measurements of $Li_3Na_3In_2F_{12}$ garnet ($Ia\bar{3}d$, $Z = 8$).

Pressure (GPa)	0.0001	0.02	1.80	2.43	3.39	4.07
Crystal data						
a (Å)	12.7070(14)	12.7049(28)	12.5212(15)	12.4664(14)	12.3895(39)	12.337(6)
V (Å^3)	2051.76(0.69)	2050.77(1.36)	1963.10(0.69)	1937.44(0.67)	1901.80(1.80)	1877.7(2.7)
ρ (g cm^{-3})	3.5431	3.5448	3.7032	3.7522	3.8225	3.8715
μ (mm^{-1})	4.770	4.772	4.985	5.051	5.146	5.212
G_{iso}	0.159(12)	0.149(11)	0.147(12)	0.142(11)	0.153(11)	0.120(13)
Data collection						
No. measured refl.	3736	3762	3479	3550	3498	3669
Range of hkl	$-15 \leqslant h \leqslant 15$	$-15 \leqslant h \leqslant 15$	$-15 \leqslant h \leqslant -14$	$-15 \leqslant h \leqslant 15$	$-15 \leqslant h \leqslant 15$	$-11 \leqslant h \leqslant 11$
	$-15 \leqslant k \leqslant 15$	$-15 \leqslant k \leqslant 15$	$-15 \leqslant k \leqslant 15$	$-15 \leqslant k \leqslant 15$	$-14 \leqslant k \leqslant 15$	$-14 \leqslant k \leqslant 14$
	$-9 \leqslant l \leqslant 9$	$-9 \leqslant l \leqslant 9$	$-9 \leqslant l \leqslant 9$	$-9 \leqslant l \leqslant 9$	$-9 \leqslant l \leqslant 9$	$-15 \leqslant l \leqslant 15$
No. unique refl.	177	177	169	166	165	164
No. observed refl.[a]	88	91	91	90	87	92
$R(\text{int})_{obs/all}$	4.98/7.45	4.91/7.10	4.86/6.58	5.05/6.87	4.96/7.08	6.26/8.58
$\sin(\theta)/\lambda$	0.619 660	0.619 763	0.623 763	0.610 905	0.614 697	0.617 313
Refinement[b]						
R_{obs}	1.95	2.04	2.21	1.90	1.91	2.84
wR_{obs}	2.47	2.35	2.83	2.48	2.36	3.48
R_{all}	6.41	7.11	6.52	6.10	5.79	7.48
wR_{all}	2.85	2.67	2.99	2.80	2.61	3.63
GoF_{all}	1.20	1.17	1.32	1.22	1.14	1.51
GoF_{obs}	1.57	1.51	1.80	1.55	1.50	2.03
No. parameters	17	17	17	17	17	17

[a] The criterion for observed reflections is $|F_{obs}| > 3\sigma$.

[b] All agreement factors are given in %; weighting scheme $1/[\sigma^2(F_{obs}) + (0.01F_{obs})^2]$.

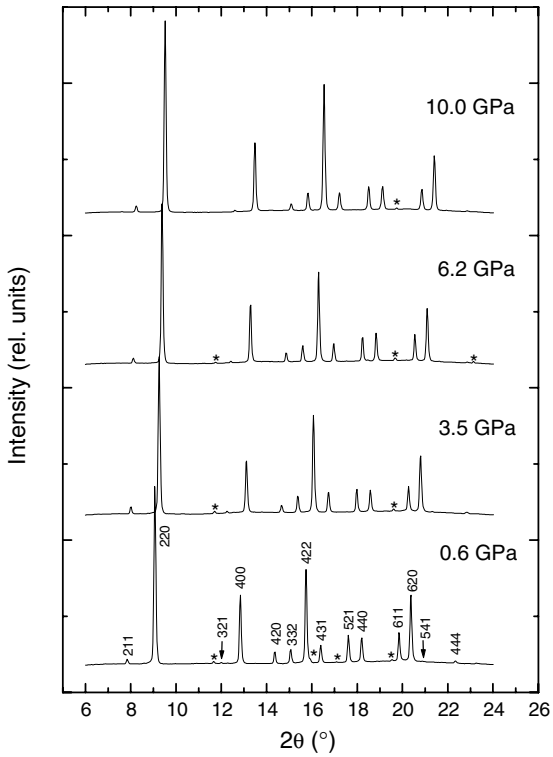

Figure 2. X-ray powder patterns of $Li_3Na_3In_2F_{12}$ garnet upon compression ($\lambda = 0.7100$ Å). Miller indices mark the reflections of the garnet. The weak reflections indicated with stars are due to the sample environment.

Table 2. Fluorine atomic positions from single-crystal refinements of $Li_3Na_3In_2F_{12}$ garnet ($Ia\bar{3}d$, $Z = 8$).

Pressure (GPa)	0.0001	0.02	1.80	2.43	3.39	4.07
x	−0.0294(2)	−0.0298(2)	−0.0305(2)	−0.0307(2)	−0.0307(2)	−0.0311(3)
y	0.0517(2)	0.0515(2)	0.0548(2)	0.0556(2)	0.0566(2)	0.0579(3)
z	0.1512(3)	0.1510(3)	0.1513(3)	0.1516(3)	0.1524(3)	0.1517(4)

neighbour cations, i.e., the bonds In–F, Li–F and the second Na–F(2), are nearly constant upon compression (figure 3). The two Na–F bonds have a tendency to become equivalent at 5.5–6.0 GPa. Figure 3 also shows relative changes of polyhedral volumes around the Li, Na, and In cations. The volumes have been calculated using the program IVTON [26]. The NaF_8 triangulated dodecahedra are the most compressible while the volume of the InF_6 octahedra is much less sensitive to external pressure.

Quantitative parameters for evaluating the polyhedral distortions in $Li_3Na_3In_2F_{12}$ at high pressures are plotted in figure 4. These parameters describe relative changes (all in %) of the angles in the LiF_4 tetrahedra, Na–F bonds in the NaF_8 triangulated dodecahedra, F–F distances and F–In–F angles in the InF_6 octahedra. The bond length distortion of the NaF_8 triangulated dodecahedra is $100|d_1 - d_2|/|d_1 + d_2|$, where d_1 and d_2 are Na–F distances. The edge length distortion of the InF_6 octahedra is $100|f_1 - f_2|/|f_1 + f_2|$, where f_1 and f_2 are F–F distances in the octahedra. The angular distortion of the LiF_4 tetrahedra is $100(|\alpha_1 - \alpha_0| + 2|\alpha_2 - \alpha_0|)/(3\alpha_0)$,

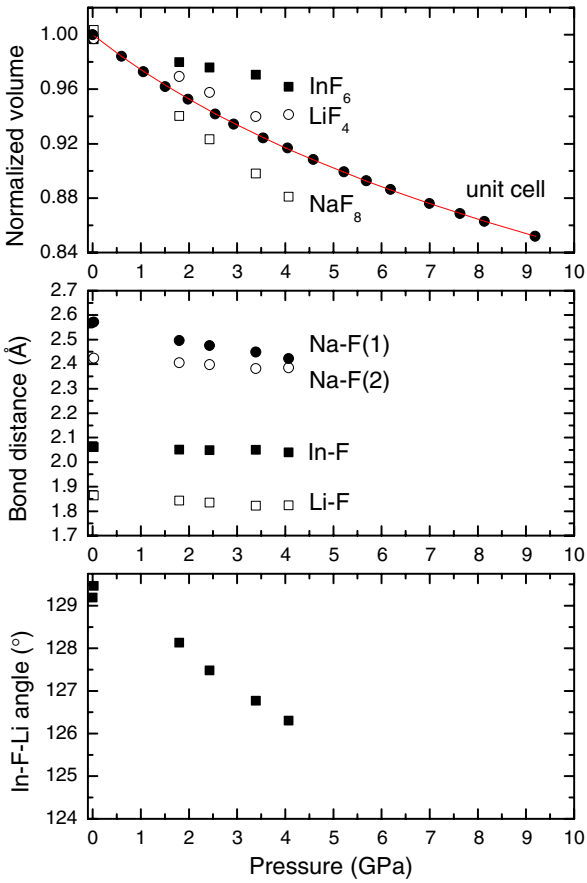

Figure 3. Pressure dependence of normalized unit-cell and polyhedral volumes, interatomic distances, and In–F–Li interpolyhedral angles in $Li_3Na_3In_2F_{12}$ garnet. The solid line represents the equation of state.

where α_1 and α_2 are tetrahedral angles, while $\alpha_0 = 109.471°$. The angular distortion of the InF_6 octahedra is $100|\beta_1 - \beta_2|/90$, where β_1 and β_2 are octahedral angles. Our data clearly demonstrate that the LiF_4 tetrahedra become more regular, while both distortion parameters for the InF_6 octahedra increase at high pressures. The bond length distortion of the NaF_8 polyhedra diminishes, but it is expected to increase above 5.5–6 GPa. Upon compression, the triangulated dodecahedra in several silicate garnets initially become more regular, but at higher pressures their distortions enhance without any structural phase transition from the $Ia\bar{3}d$ ($Z = 8$) symmetry [18, 19].

The compression features in $Li_3Na_3In_2F_{12}$ (figures 3 and 4) generally agree with the respective pressure-induced changes in the structural parameters in silicate garnets [18, 19], apart from the fact that the tetrahedral units in the silicates are the least compressible. The change of the angle M′–O–M‴ between the $M'O_4$ tetrahedra and $M'''O_6$ octahedra in silicate garnets of about 6° at 100 GPa [19], with their bulk moduli greater than 150 GPa, is much smaller than that in $Li_3Na_3Ga_2F_{12}$.

The same polyhedral distortion parameters are calculated from the ambient pressure structural data for $Li_3Na_3Al_2F_{12}$ [4] and $Li_3Na_3Fe_2F_{12}$ [8], the two structures which have been

Table 3. Displacement parameters from single-crystal refinements of $Li_3Na_3In_2F_{12}$ garnet ($Ia\bar{3}d$, $Z = 8$).

	U_{11}	U_{22}	U_{33}	U_{12}	U_{13}	U_{23}	U_{iso}
0.0001 GPa							
Li	—	—	—	—	—	—	0.014(5)
Na	0.024(2)	0.014(3)	U_{11}	0	0.006(2)	0	0.021(1)
In	0.0139(2)	U_{11}	U_{11}	−0.0014(3)	U_{12}	U_{12}	0.0139(2)
F	0.015(2)	0.024(2)	0.012(2)	−0.005(2)	0.006(1)	−0.002(2)	0.017(1)
0.02 GPa							
Li	—	—	—	—	—	—	0.011(4)
Na	0.026(2)	0.018(3)	U_{11}	0	0.006(2)	0	0.023(1)
In	0.0141(3)	U_{11}	U_{11}	−0.0013(3)	U_{12}	U_{12}	0.0141(2)
F	0.017(2)	0.023(2)	0.012(2)	−0.007(1)	0.005(1)	−0.006(1)	0.017(1)
1.80 GPa							
Li	—	—	—	—	—	—	0.015(5)
Na	0.019(2)	0.014(3)	U_{11}	0	0.003(2)	0	0.017(1)
In	0.0136(4)	U_{11}	U_{11}	−0.0015(3)	U_{12}	U_{12}	0.0136(2)
F	0.017(2)	0.021(2)	0.013(2)	−0.006(2)	0.005(1)	−0.002(2)	0.017(1)
2.43 GPa							
Li	—	—	—	—	—	—	0.016(5)
Na	0.019(2)	0.013(2)	U_{11}	0	0.005(2)	0	0.017(1)
In	0.0132(3)	U_{11}	U_{11}	−0.0015(3)	U_{12}	U_{12}	0.0132(2)
F	0.015(2)	0.022(2)	0.012(2)	−0.008(1)	0.003(1)	−0.001(1)	0.016(1)
3.39 GPa							
Li	—	—	—	—	—	—	0.022(5)
Na	0.018(2)	0.014(2)	U_{11}	0	0.003(2)	0	0.016(1)
In	0.0136(3)	U_{11}	U_{11}	−0.0015(3)	U_{12}	U_{12}	0.0136(2)
F	0.017(2)	0.021(2)	0.014(2)	−0.007(1)	0.005(1)	−0.002(1)	0.017(1)
4.07 GPa							
Li	—	—	—	—	—	—	0.017(7)
Na	0.014(4)	0.017(2)	U_{11}	0	0.003(3)	0	0.016(2)
In	0.0124(4)	U_{11}	U_{11}	−0.0015(4)	U_{12}	U_{12}	0.0124(2)
F	0.014(3)	0.014(3)	0.012(2)	−0.006(2)	0.004(2)	−0.001(1)	0.013(2)

fully refined from single-crystal data. They are compared with the parameters for $Li_3Na_3In_2F_{12}$ at 0.0001 GPa (this study) and plotted as a function of the effective ionic radius [27] of the Me^{3+} cation at the octahedral site in figure 5 (Me^{3+}: Al^{3+}, Fe^{3+}, In^{3+}). Unlike those in the NaF_8 bisdisphenoids, the distortions in the LiF_4 and MeF_6 polyhedra increase with increasing effective radii. The Me^{3+} ionic radius effect on the distortion of the MeF_6 octahedra (figure 5) corresponds to the influence of external pressure on the distortions of the InF_6 octahedra in $Li_3Na_3In_2F_{12}$ (figure 4). At atmospheric conditions, the unit-cell volumes for $Li_3Na_3Al_2F_{12}$ [4], $Li_3Na_3Fe_2F_{12}$ [8], and $Li_3Na_3In_2F_{12}$ (this study) are 1781.24, 1900.63, and 2051.76(0.69) $Å^3$, while the Me–F–Li angles are 136.10°, 132.75°, and 129.19(16)°, respectively.

4. Discussion

Our observations provide evidence that $Li_3Na_3In_2F_{12}$ garnet ($Ia\bar{3}d$, $Z = 8$) remains structurally stable to at least 9.2 GPa. The increase in the exponential lifetime of the $^4T_2$ emission in the Cr^{3+} luminescence spectra [12] correlates very well with the increasing distortions of the InF_6 octahedra that are the least compressible polyhedra in the structure (figures 3 and 4). Upon compression, the compound studied here becomes a garnet with

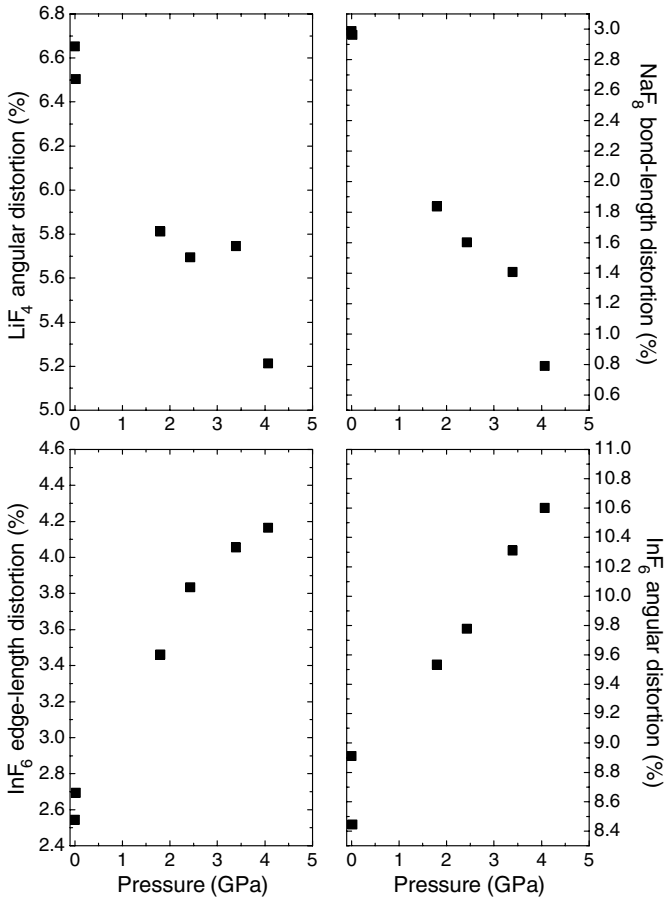

Figure 4. Pressure dependence of angular, bond length, and edge length distortions in LiF_4, InF_6, and NaF_8 polyhedra in $Li_3Na_3In_2F_{12}$ garnet.

a 'large' octahedral cation, since the effective $r(In^{3+})/r(F^{1-})$ ratio increases due to the compressibility of the 'soft' F^{1-} anion as well as of the Na^{1+} and Li^{1+} cations.

The bulk modulus of $Li_3Na_3In_2F_{12}$ ($Ia\bar{3}d$, $Z = 8$) is very small, $B_0 = 36.2(5)$ GPa, and comparable to the moduli of oxide hydrogarnets [18, 19]. It is one order of magnitude lower than the moduli of silicate garnets. It is the large compressibility of the LiF_4 tetrahedra that dictates comparisons with hydrogarnets and not classical garnets. The most compressible polyhedral units in $Li_3Na_3In_2F_{12}$ are the NaF_8 triangulated dodecahedra (figure 3). However, the exact reason why the trilithium trisodium diindium fluoride is so soft is the massive folding of its tetrahedral–octahedral framework (figures 1 and 4).

5. Conclusions

Our x-ray diffraction experiments show that there is no pressure-induced phase transition in $Li_3Na_3In_2F_{12}$ garnet ($Ia\bar{3}d$, $Z = 8$) to 9.2 GPa. Its small bulk modulus $B_0 = 36.2(5)$ GPa is explained by the large change of the Li–F–In angle between the LiF_4 tetrahedra and InF_6 octahedra.

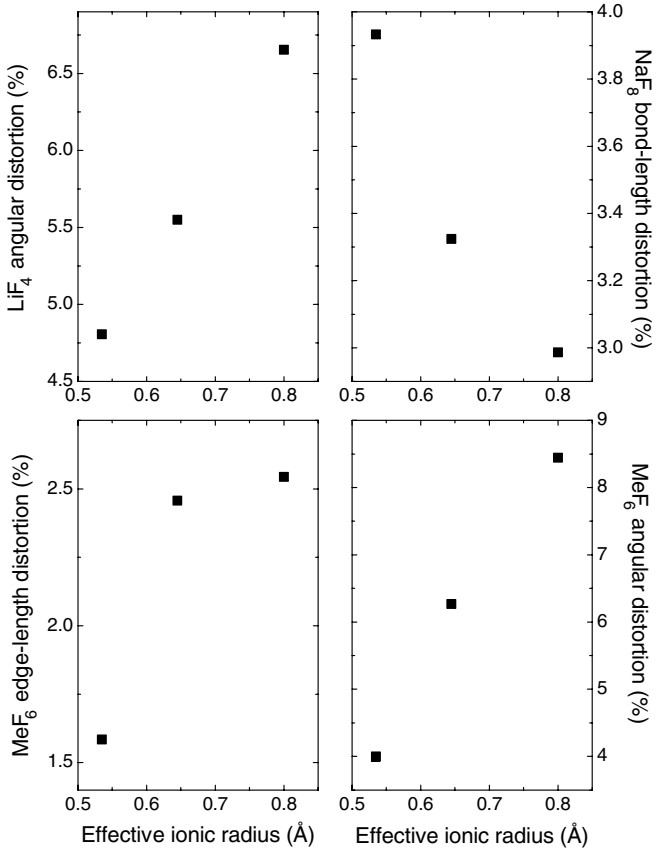

Figure 5. Angular, bond length, and edge length distortions in LiF_4, MeF_6, and NaF_8 polyhedra in $Li_3Na_3Al_2F_{12}$ [4], $Li_3Na_3Fe_2F_{12}$ [8], and $Li_3Na_3In_2F_{12}$ (this study) at ambient pressure as a function of the effective Me^{3+} ionic radius; $r(Al^{3+}) = 0.535$ Å, $r(Fe^{3+}) = 0.645$ Å, $r(In^{3+}) = 0.800$ Å [27].

Acknowledgments

The x-ray powder data were collected during the HS-2179 beamtime at the European Synchrotron Radiation Facility (Grenoble). Experimental assistance from the staff of the Swiss–Norwegian Beamlines at ESRF is gratefully acknowledged. We also acknowledge financial support from the Ministerio de Ciencia y Tecnología, the Gobierno Vasco, and the Danish National Research Council.

References

[1] Wells A F 1984 *Structural Inorganic Chemistry* 5th edn (Oxford: Oxford University Press)
[2] de Pape R, Portier J, Gauthier G and Hagenmuller P 1967 *C. R. Acad. Sci., Paris* C **265** 1244
[3] de Pape R, Portier J, Grannec J, Gauthier G and Hagenmuller P 1969 *C. R. Acad. Sci., Paris* C **269** 1120
[4] Geller S 1971 *Am. Mineral.* **56** 18
[5] Morell A, Tanguy B, Portier J and Hagenmuller P 1974 *J. Fluorine Chem.* **3** 351
[6] Tekeda Y, Sone M, Suwa Y, Inagaki M and Naka S 1977 *J. Solid State Chem.* **20** 261
[7] Langley R H and Sturgeon G D 1979 *J. Fluorine Chem.* **14** 1

[8] Massa W, Post B and Babel D 1982 *Z. Kristallogr.* **158** 299
[9] Chamberlain S and Corruccini L R 1997 *J. Phys. Chem. Solids* **58** 899
[10] de Viry D, Denis J P, Blanzat B and Grannec J 1987 *J. Solid State Chem.* **71** 109
[11] de Viry D, Pellé F, Denis J P, Blanzat B, Grannec J and Chaminade J P 1987 *J. Fluorine Chem.* **35** 244
[12] de Viry D, Denis J P, Tercier N and Blanzat B 1987 *Solid State Commun.* **63** 1183
[13] Caird J A, Payne S A, Staver P R, Ramponi A J, Chase L L and Krupke W F 1988 *IEEE J. Quantum Electron.* **24** 1077
[14] de Viry D, Casalboni M and Palumno M 1990 *Solid State Commun.* **76** 1051
[15] de Viry D, Pilla O, Pellé F and Blanzat B 1991 *J. Lumin.* **48/49** 561
[16] Aramburu J A, Barriuso M T and Moreno M 1996 *J. Phys.: Condens. Matter* **8** 6901
[17] Machado M A C, Pachoal C W A, Mendes Filho J, Ayala A P, Moreira R L and Gesland J-Y 2002 *J. Phys.: Condens. Matter* **14** 271
[18] Hazen R M and Finger L W 1989 *Am. Mineral.* **74** 352
[19] Akhmatskaya E V, Nobes R H, Milman V and Winkler B 1999 *Z. Kristallogr.* **214** 808
Milman V, Akhmatskaya E V, Nobes R H, Winkler B, Pickard C J and White J A 2001 *Acta Crystallogr.* B **57** 163
[20] Hammersley A P, Svensson S O, Hanfland M, Fitch A N and Häusermann D 1996 *High Pressure Res.* **14** 235
[21] Piermarini G J, Block S, Barnett J D and Forman R A 1975 *J. Appl. Phys.* **46** 2774
Mao H K, Xu J and Bell P M 1986 *J. Geophys. Res.* **91** 4673
[22] Bruker (2000), Bruker AXS Inc., Madison, Wisconsin
[23] Angel R J, Allan D R, Miletich R and Finger L W 1997 *J. Appl. Crystallogr.* **30** 461
[24] Petricek V, Dusek M and Palatinus L 2000 *The Crystallographic Computing System* (Praha: Institute of Physics)
[25] Becker P J and Coppens P 1974 *Acta Crystallogr.* A **30** 129
[26] Balic-Zunic T and Vickovic I 1996 *J. Appl. Crystallogr.* **29** 305
[27] Shannon R D 1976 *Acta Crystallogr.* A **32** 751